JOURNAL OF VIROLOGY, Feb. 2008, p. 1701–1713 Vol. 82, No. 4
0022-538X/08/$08.00+0 doi:10.1128/JVI.02157-07

Translocation and Colocalization of ICP4 and ICP0 in Cells Infected with Herpes Simplex Virus 1 Mutants Lacking Glycoprotein E, Glycoprotein I, or the Virion Host Shutoff Product of the U_L41 Gene[▽]

Maria Kalamvoki, Jianguo Qu, and Bernard Roizman*

Marjorie B. Kovler Viral Oncology Laboratories, The University of Chicago, 910 East 58th Street, Chicago, Illinois 60637

Received 2 October 2007/Accepted 20 November 2007

In wild-type herpes simplex virus 1-infected cells, the major regulatory protein ICP4 resides in the nucleus whereas ICP0 becomes dynamically associated with proteasomes and late in infection is translocated and dispersed in the cytoplasm. Inhibition of proteasomal function results in retention or transport of ICP0 to the nucleus. We report that in cells infected with mutants lacking glycoprotein E (gE), glycoprotein I (gI), or the product of the U_L41 gene, both ICP4 and ICP0 are translocated to the cytoplasm and coaggregate in small dense structures that, in the presence of proteasomal inhibitor MG132, also contain proteasomal components. Gold particle-conjugated antibody to ICP0 reacted in thin sections with dense protein aggregates in the cytoplasm of mutant virus-infected cells. Similar aggregates were present in the nuclei but not in the cytoplasm of wild-type virus-infected cells. Exposure of cells early in infection to MG132 does not result in retention of ICP0 as in wild-type virus-infected cells. The results suggest that the retention of ICP4 and ICP0 in the nucleus is a dynamic process that involves the function of other viral proteins that may include the Fc receptor formed by the gE/gI complex and is not merely the consequence of expression of a nuclear localization signal. It is noteworthy that in ΔU_L41-infected cells gE is retained in the *trans*-Golgi network and is not widely dispersed in cellular membranes.

In an earlier study concerning the redistribution of the IP3 receptor I in infected cells, we noted that the infected cell protein no. 4 (ICP4) is translocated into the cytoplasm in cells infected with mutant viruses lacking glycoprotein E or U_L41, the gene encoding the virion host shutoff protein (vhs) (18). This was an unexpected finding. ICP4 is one of several major regulatory proteins encoded by herpes simplex virus 1 (HSV-1). The protein acts both as a repressor and as a transactivator. Studies of temperature-sensitive mutants have shown that ICP4 is required throughout the replicative cycle of the virus (5, 6). Unlike ICP0, which late in infection with wild-type virus is translocated to the cytoplasm, ICP4 is thought to be a nuclear protein and in fact resides exclusively in the nucleus in wild-type virus-infected cells. This report centers on the role of gE, gI, and U_L41 proteins in the localization of ICP4 and ICP0 proteins. Relevant to this report are the following.

(i) In wild-type virus-infected cells, there is not significant colocalization of ICP0 and ICP4. ICP0 initially colocalizes with the ND10 structure (12, 30, 31), fills the nucleus, and eventually, between 9 and 12 h after infection, is present in a diffuse form entirely in the cytoplasm (16, 19, 20, 28). Export of ICP0 to the cytoplasm is blocked by exposure of cells 2 h after infection to proteasomal inhibitor MG132 (13, 28). A striking feature of the translocation process is that exposure of infected cells to MG132 after ICP0 has been exported to the cytoplasm results in the relocation of ICP0 to the nucleus (28).

ICP0 is also exported to the cytoplasm in cells infected with mutants lacking ICP4 (ΔICP4) (16, 28). Unlike the situation with wild-type virus-infected cells, ICP0 is translocated at earlier times after infection and forms small dense structures dispersed throughout the cytoplasm or arranged around the nucleus. In the presence of MG132, added late after infection, ICP0 is retained in the cytoplasm in similar small dense structures that also contain proteasomal components (28). Relevant to this report is the observation that a D199A substitution in ICP0 prevents the translocation of ICP0 to the cytoplasm (52, 53). This observation suggests that the translocation of ICP0 is an active process involving an interactive partner.

Last, ICP0 and ICP4 have been reported to colocalize in the cytoplasm in cells transfected with plasmids encoding the two proteins (35).

(ii) Although the focus of numerous publications has been on gE, this glycoprotein most likely exists in a complex with gI. A key property of this complex is that of an Fc receptor. gE consists of an ~396-residue ectodomain, a 25-residue transmembrane domain, and a 106-residue cytoplasmic domain (40). gI consists of a 248-residue ectodomain, a transmembrane domain, and a 94-residue cytoplasmic domain (47). gE and gI form a heterodimer. The gE domains required for association with gI and binding with immunoglobulin G (IgG) are in the ectodomain (2, 3, 4, 40). Both gE and gI cytoplasmic domains contain amino acid motifs associated with endocytosis, and both glycoproteins are highly phosphorylated by both viral and cellular kinases (1, 4, 34, 37, 54).

The phenotypic properties of the gE/gI complex have been

* Corresponding author. Mailing address: Marjorie B. Kovler Viral Oncology Laboratories, The University of Chicago, 910 East 58th Street, Chicago, IL 60637. Phone: (773) 702-1898. Fax: (773) 702-1631. E-mail: bernard.roizman@bsd.uchicago.edu.

▽ Published ahead of print on 5 December 2007.

studied extensively. gE/gI shuttles between the cell surface and the *trans*-Golgi network (4, 14, 32). A rich and persuasive literature has linked the gE/gI complex to cell-to-cell spread of virus. In experimental animals, the gE/gI complex plays a key role in neuronal spread across synapses (7, 8). The complex is not involved in virus entry or cell-cell fusion. Its action may well be to facilitate the delivery of virion cargo from the site of cytoplasmic envelopment to the cell surface (39). It has also been proposed that the binding of IgG by the Fc receptor diverts the immune system from cell destruction by antibody and complement (17, 29, 36, 51).

(iii) The U_L41 protein, also known as the virion host shutoff protein, is an endoribonuclease that is active primarily early in infection upon entry of the virus into the cell. The U_L41 protein of HSV-1 degrades RNA by endonucleolytic cleavage in the absence of other cellular or viral proteins (22, 46, 48, 50).

U_L41 is expressed late in the replicative cycle. The newly synthesized U_L41 protein is in complexes with VP16 and VP22 and is not active as a nuclease (21, 23, 45, 49). Numerous studies have linked components of the Fc receptor with members of the U_L41/VP16/VP22 complex or other viral proteins. Specifically, the cytoplasmic domain of gE interacts with a conserved domain of VP22 (38). The interaction takes place in infected cells, since VP22 as well as U_L11 was precipitated in connection with full-length gE/gI and also with gD from HSV-1-infected cells (15). HSV-1 ΔVP22 mutants incorporate reduced amounts of gB, gD, and gE into the virion envelope (9, 11). It is noteworthy, however, that ΔVP22 mutants lack functional U_L41 protein (44). In essence, in the course of the replicative cycle, the gE/gI complex interacts with various tegument proteins that include VP22 and by extension the product of the U_L41 gene.

MATERIALS AND METHODS

Cells and viruses. HEp-2 cells, obtained from the American Type Culture Collection (Rockville, MD), and telomerase-transformed human embryonic lung (HEL) fibroblasts, obtained from T. Shenk (Princeton), were grown in Dulbecco's modified Eagle medium supplemented with 10% fetal bovine serum. Rabbit skin cells (RSC) were originally obtained from J. McClaren and were maintained in 5% fetal bovine serum. Human 143 thymidine kinase-negative ($143TK^-$) cells were originally obtained from Carlo Croce and were maintained in 5% newborn calf serum.

HSV-1(F), a limited-passage isolate, is the prototype strain used in this laboratory (10). R7032 (ΔgE-2), a recombinant virus with a HincII-NruI deletion in the coding sequence for the U_S8 and $U_S8.5$ genes, has been reported previously (33). R7030 (ΔgE-1), a recombinant virus that contains an insertion of the chimeric α27-TK gene into the unique HpaI site of the gE gene, has been described elsewhere (26). The construction and properties of the ΔU_L41 (ΔVHS) mutant virus R2621 were reported elsewhere (41). The HSV-1 (KOS)d120 mutant, a kind gift of N. DeLuca, lacks both copies of the α4 gene and was grown in a Vero-derived cell line (E5) expressing the α4 gene. It also does not express the U_S3 gene (25).

Plasmid construction. The plasmid pRB123, which carries a 6,584-bp BamHI J fragment (42), was digested to completion with the BstEII enzyme to delete domains of the U_S7 (gI) and U_S8 (gE) genes. The DNA was selfligated to generate the plasmid designated pRB123-BstEII collapsed. The 1,311-bp fragment from the pRB123/BstEII digest, which carries sequences from the U_S8 gene and only the carboxyl-terminal domain from the U_S7 protein, was ligated back to the pRB123-BstEII collapsed plasmid to generate the plasmid designated pΔgI, which carries a repaired U_S8 gene (as in pRB123) and a 531-bp deletion in the U_S7 (gI) coding sequence.

Construction of recombinant viruses. Recombinant R7081 was constructed by cotransfection of rabbit skin cells with intact R7030 (ΔgE-1) viral DNA and the pΔgI plasmid. TK^- progeny viruses were selected on $143TK^-$ cells overlaid with Dulbecco's modified Eagle medium containing 5% newborn calf serum and 40 μg of bromodeoxyuridine per ml of medium, as described previously (43). The recombinant viruses were plaque purified after two rounds of selection, and their purity was verified by PCR amplification of the entire gI coding sequence, which was expected to be 531 bp shorter than that of the wild-type gene. The restoration of gE protein expression and the abrogation of gI protein expression from the progeny virus were confirmed by immunoblot analysis, as detailed in Results.

Immunofluorescence analysis. The immunofluorescence studies were done as described earlier (18), with minor modifications. Briefly, cells grown on four-well slides were exposed for 2 h to 10 PFU of wild-type or mutant viruses per cell. For the experiments with MG132 (Biomol), the drug was added to the cultures at a final concentration of 5 μM after 2 h of absorption. Cells were fixed in 4% paraformaldehyde and, at the indicated time after infection, neutralized with 100 mM glycine in phosphate-buffered saline (PBS), permeabilized/blocked with 0.1% Triton X-100 in PBS in the presence of 20% horse serum and 1% bovine serum albumin (BSA) (PBS-TBH solution), and reacted with primary antibodies diluted in PBS-TBH, as described earlier (18). The ICP4 and ICP0 mouse monoclonal antibodies (Goodwin Institute for Cancer Research, Plantation, FL) and the ICP0 exon 2 rabbit polyclonal antibody (20) were used in a dilution of 1:2,000. The rabbit polyclonal antibody against the 20S proteasome core subunits (PW 8155; Affiniti Research Products Ltd., Mamhead, Exeter, Devon, United Kingdom) was used in a dilution of 1:3,000. The TGN46 rabbit polyclonal antibody (Abcam, Inc.) was used in a dilution of 1:500. The gE mouse monoclonal antibody (clone 1108; Goodwin Institute for Cancer Research, Plantation, FL) was used in a dilution of 1:500. Following this incubation, the samples were rinsed several times with PBS-TBH and reacted with the proper secondary antibody, Alexa Fluor 594-conjugated goat anti-rabbit or Alexa Fluor 488-conjugated goat anti-mouse, diluted 1:1,000 in PBS-TBH. Finally, after several rinses first with PBS-TBH and then with PBS, the samples were mounted in Vectashield mounting medium for fluorescence (Vector Laboratories) and examined with a Zeiss confocal microscope equipped with software provided by Zeiss.

Immunoblot analysis. Protein preparation and immunoblotting were done as detailed elsewhere (18). Briefly, replicate cell cultures in six-well plates were either mock infected or exposed to 10 PFU of virus per cell in 199V medium (Sigma) at 37°C. The cells were harvested at the indicated times after infection, rinsed with PBS, solubilized in triple detergent buffer (50 mM Tris-HCl [pH 8], 150 mM NaCl, 0.1% sodium dodecyl sulfate, 1% Nonidet P-40, 0.5% sodium deoxycholate, 100 $\mu g\ ml^{-1}$ of phenylmethylsulfonyl fluoride) supplemented with phosphatase inhibitors (10 mM NaF, 10 mM β-glycerophosphate, 0.1 mM sodium vanadate) and protease inhibitor cocktail (Sigma) as specified by the manufacturer, and briefly sonicated. The protein concentration in total cell lysates was determined with the aid of a Bio-Rad protein assay (Bio-Rad Laboratories), according to directions provided by the supplier. Approximately 70 μg of proteins per sample was subjected to further analysis.

Proteins were electrophoretically separated in denaturing polyacrylamide gels, electrically transferred to a nitrocellulose sheet, blocked with PBS supplemented with 0.02% (vol/vol) Tween 20 (PBST) and 5% nonfat milk, and reacted overnight at 4°C with the appropriate primary antibodies diluted in PBST-1% nonfat milk. The mouse monoclonal antibodies for ICP4, ICP0, and ICP8 (Goodwin Institute for Cancer Research, Plantation, FL) were used in a dilution of 1:1,000. The gI mouse monoclonal antibody (clone Fd69) (27) was used in a dilution of 1:250. The gE mouse monoclonal antibody (clone 3114), kindly provided by D. Johnson, was used in a dilution of 1:500. The anti-U_L41 rabbit polyclonal antibody has been described before (50) and was used in a dilution of 1:1,000. The U_L38 rabbit polyclonal antibody was purchased from the Goodwin Institute for Cancer Research and was used in a dilution of 1:1,000. The β-actin mouse monoclonal antibody (Sigma) was used in a dilution of 1:2,000. After several rinses with PBST-1% nonfat milk, the membranes were reacted with the appropriate secondary antibody conjugated to alkaline phosphatase. Finally, protein bands were visualized with 5-bromo-4-chloro-3-indolylphosphate (BCIP)–nitroblue tetrazolium (Denville Scientific, Inc.).

[^{35}S]methionine labeling of infected cells. Replicate cultures in 25-cm^2 flasks were either mock infected or exposed to 10 PFU of virus per cell and incubated at 37°C. At 7, 9, and 11 h after infection, the cells were rinsed with methionine-free, serum-free 199 medium (Sigma) and overlaid with 1 ml of this medium supplemented with 100 μCi of [^{35}S]methionine (specific activity, >1,000 Ci/mmol; Perkin Elmer Life Sciences) for 1 h. The cells were harvested and solubilized, and approximately 100 μg of total proteins per sample was subjected to electrophoresis in an 8% denaturing polyacrylamide gel, transferred to a nitrocellulose sheet as described above, and subjected to autoradiography.

Electron microscopy. HEp-2 cells were harvested at 18 h after infection with 10 PFU of either the HSV-1(F) or the ΔgE-2 virus per cell, rinsed with serum-free culture medium, and fixed in 4% paraformaldehyde-0.15% glutaraldehyde in 0.1 M PB buffer (76.7 mM Na_2HPO_4, 26.4 mM NaH_2PO_4, pH 7.4) for 1 h. The

fixed cells were rinsed three times for 20 min each with 0.1 M PB on ice and dehydrated in a graded ethanol series (30, 50, 70, 95, and 3× 100% ethanol in water) at 4°C (30 and 50%) and at room temperature (70, 95, and 3× 100%) for 15 min per step. Subsequently, the cells were infiltrated using a mixture of LR White medium (London Resin Company Limited) with 100% ethanol, 1:1, followed by infiltration with pure LR White medium overnight and five 1-h changes with pure LR White medium the next day. All infiltrations were done at room temperature. After infiltration, cells were polymerized in a vacuum oven at 45°C for 48 h. Ultrathin sections of the embedded cells, 80 nm, were made using a diamond knife (Reichert-Jung Ultra-cut E) and collected on Formvar-coated 200-mesh nickel grids.

For immunogold labeling, sections collected on grids were rehydrated with PBS for 30 min, blocked with 1% BSA in PBS for 30 min, and incubated with diluted ICP0 rabbit polyclonal antibody (e.g., 1:100, 1:500, 1:1,000, and 1:2,000 in 1% BSA in PBS) in a humidified chamber for 3.5 h at room temperature. Following incubation, the sections were washed six times for 10 min each with PBS, blocked again with 0.5% BSA in PBS for 25 min, and incubated with 10-nm colloidal gold-conjugated goat anti-rabbit IgG (heavy plus light chains; Ted Pella) diluted 1:10 in 0.5% BSA in PBS for 1 h in a humidified chamber at room temperature. Finally, the sections were washed with PBS three times for 10 min each, fixed with 1% glutaraldehyde in PBS for 10 min, aqua washed three times for 5 min each, stained briefly with uracyl acetate and lead citrate, air dried, and examined under a Siemens 102 electron microscope.

RESULTS

Properties of the ΔgE, ΔgI, and ΔU$_L$41 viruses. In wild-type HSV-1-infected cells, ICP4 accumulates exclusively in the nucleus. In earlier studies, we noted that ICP4 accumulated in the cytoplasm of cells infected with ΔgE or ΔU$_L$41 mutant virus (18). To further investigate this phenomenon, three series of experiments were done.

The objective of the first series of experiments centered on the role of gE and gI. In wild-type virus-infected cells, gE and gI form a complex, and it is generally thought that they function as a complex (2, 3, 7, 8). The question we addressed is whether ICP4 was translocated to the cytoplasm also in the absence of gI. For this purpose, we constructed a recombinant virus that lacks only the gI coding sequence. Figure 1 shows a schematic representation of procedures employed for this purpose. As the parent virus, we used ΔgE-1 (R7030) (26). In this mutant, the coding sequence of gE was disrupted by the insertion into the unique HpaI site of the thymidine kinase open reading frame, driven by the α27 promoter (Fig. 1, line 6). In the next step, we repaired the gE coding sequence in ΔgE-1 and simultaneously introduced a deletion of 531 bp in the gI coding sequence (Fig. 1, line 8). This recombinant was designated R7081.

Unlike the gE-2 mutant used in the earlier study, ΔgE-1 contains an intact U$_S$8.5 gene. In most studies described in this report, we tested both recombinants and found them to give identical results.

In the second series of experiments, we examined the expression of gE and gI in cells infected with wild-type, ΔgE, ΔgI, or ΔU$_L$41 virus. The cells were harvested at 18 h after infection, solubilized, subjected to electrophoresis in denaturing gels, transferred to a membrane, and probed with antibody to gE or gI. The results were as follows.

In wild-type virus-infected cells, gE formed two fast-migrating, relatively sharp bands and a slow-migrating broad band (Fig. 2A, lane 2). In ΔU$_L$41 mutant virus-infected cells, the intensity of the two faster-migrating, sharp bands was decreased and the broad, slower-migrating band was more intense and migrated faster than that of the wild-type counterpart (Fig. 2A, lane 3). It would appear that gE is processed differently in the absence of U$_L$41.

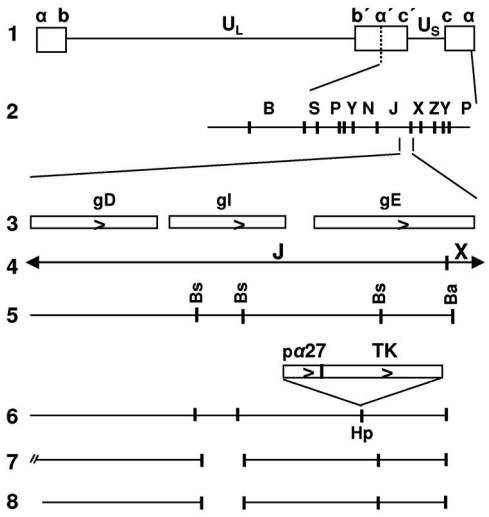

FIG. 1. Construction of the ΔgI mutant virus. Schematic representations of the DNA sequence arrangements in HSV-1(F) and of the viral recombinants and plasmids used in these studies. Line 1, sequence arrangement of the HSV-1(F) genome. Boxes represent the terminal sequences repeated internally in inverted orientation and dividing the genome into the long (U$_L$) and short (U$_S$) components. Line 2, BamHI restriction endonuclease map of HSV-1(F) DNA in the prototype (P) arrangement. Line 3, coding domains of gD, gI, and gE genes. Line 5, restriction endonuclease maps for the BamHI J and X DNA fragments shown in line 4 (Bs, BstEII; Ba, BamHI). Line 6, unique HpaI (Hp) site into which the α27-TK gene fusion was inserted, interrupting the coding domain of the gE gene. Line 7, sequence arrangement of the pΔgI plasmid, from which the 531-bp BstEII subfragment of the gI coding sequence has been deleted. Line 8, DNA sequence arrangement of the progeny ΔgI virus, R7081, with a deletion of 531 bp in the gI coding sequence.

The electrophoretic pattern of gE present in lysates of cells infected with the ΔgI mutant virus resembled to some extent that of gE in lysates of cells infected with the ΔU$_L$41 mutant virus. In brief, there was a decrease in the intensity of the two faster-migrating sharp bands. The diffuse, slow-migrating band became significantly broader and migrated faster (Fig. 2C, lane 5).

In wild-type virus-infected cells, gI forms two relatively sharp bands (Fig. 2B, lane 2). Both ΔgE mutants yielded patterns of migration of gI very similar to those of gI in lysates of wild-type virus-infected cells (Fig. 2B, lanes 4 and 5, and C, lanes 3 to 4). gI present in lysates of ΔU$_L$41 mutant-infected cells formed a third, faster-migrating double band readily visible in lighter exposures (Fig. 2B, lane 3). It would appear that gI is also processed differently in the absence of U$_L$41 than in the wild-type virus-infected cells.

Last, it was of interest to determine whether cells infected with mutant viruses differed with respect to the synthesis of viral proteins at approximately the time of translocation of ICP0 and ICP4 from the nucleus to the cytoplasm. In these experiments, HEL cells were mock infected or exposed to 10 PFU of wild-type, ΔgE, ΔgI, or ΔU$_L$41 virus per cell. At 7, 9, or 11 h after infection, the cells were rinsed extensively and labeled for 1 h with [^{35}S]methionine, as detailed in Materials and

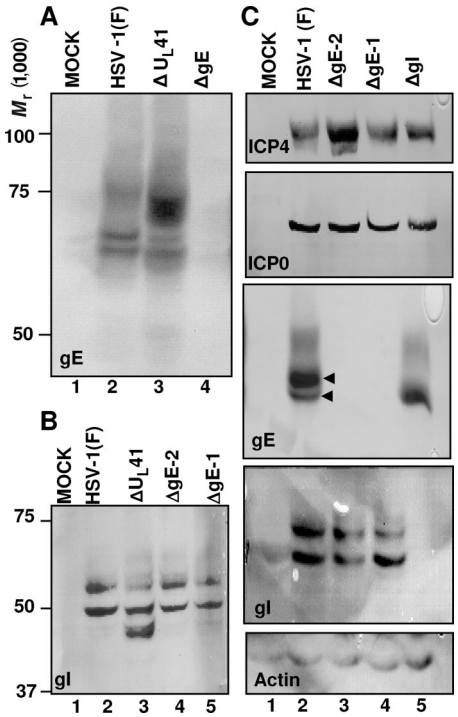

FIG. 2. Properties of the ΔgE, ΔgI, and ΔU_L41 viruses. (A and B) Expression patterns of gE and gI in ΔU_L41 virus-infected cells. HEp-2 cells were either mock infected or exposed (10 PFU/cell) to HSV-1(F), ΔU_L41, ΔgE-2 (R7032), or ΔgE-1 (R7030) mutant viruses. The cells were harvested at 18 h after infection and lysed, and equal amounts of proteins were electrophoretically separated on 7% (A) or 10% (B) denaturing polyacrylamide gels, transferred to nitrocellulose sheets, and immunoblotted with either the gE (clone 3114) (A) or the gI (B) mouse monoclonal antibody, as detailed in Materials and Methods. (C) Characterization of the ΔgI mutant virus. HEL cells were either mock infected or exposed (10 PFU/cell) to HSV-1(F), ΔgE-2 (R7032), ΔgE-1 (R7030), or ΔgI mutant viruses. Cells were harvested at 18 h after infection and lysed, and equal amounts of protein were separated on replicate 7% or 10% denaturing polyacrylamide gels. The electrophoretically separated proteins were transferred to nitrocellulose sheets and reacted with the gE (clone 3114), gI, ICP4, or ICP0 mouse monoclonal antibody, as detailed in Materials and Methods. The reaction with the β-actin antibody served as a loading control.

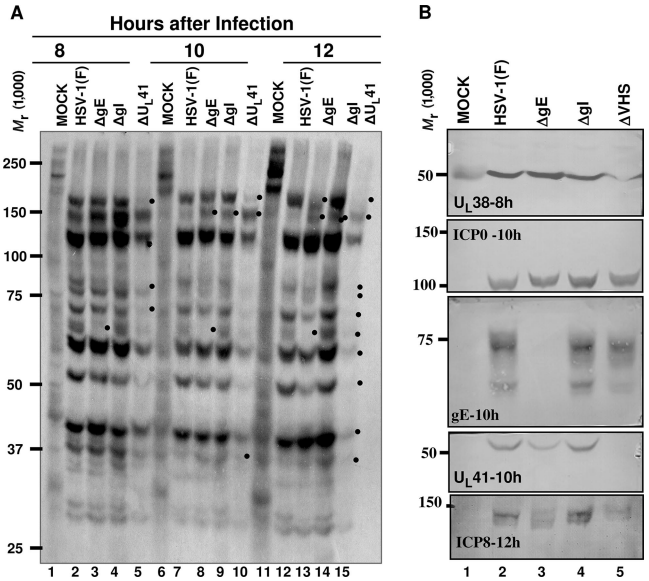

FIG. 3. Viral protein synthesis in ΔU_L41-, ΔgE-, or ΔgI-infected cells. (A) HEL cells grown in 25-cm^2 flasks were either mock infected or exposed (10 PFU/cell) to HSV-1(F), ΔgE, ΔgI, or ΔU_L41 mutant viruses. At 7, 9, or 11 h after infection, the cells were rinsed extensively with L-methionine-free, serum-free 199 medium and overlaid with the same medium supplemented with 100 μCi [^{35}S]methionine for 1 h. The cells were harvested at 8, 10, and 12 h postinfection and solubilized, and the proteins were electrophoretically separated on an 8% denaturing polyacrylamide gel, transferred to nitrocellulose, and subjected to autoradiography, as detailed in Materials and Methods. Dots shows viral proteins synthesized with different kinetics in the viruses tested. (B) After autoradiography, the nitrocellulose membrane shown in panel A was cut and immunoblotted for the U_L38, ICP0, gE, U_L41, or ICP8 protein.

Methods. Cells were then harvested, solubilized, transferred to a membrane, and subjected to autoradiography (Fig. 3A). After the autoradiographic images were collected, the membrane was cut and reacted with antibodies to ICP0, ICP8, U_L38, gE, and U_L41 (Fig. 3B). Examination of the autoradiographic images suggests that with minor exceptions the patterns of protein synthesis in cells infected with wild-type virus, ΔgE, or ΔgI at 7, 9, and 11 h after infection were very similar. In contrast, in cells infected with the ΔU_L41 mutant virus, the synthesis of proteins was much reduced and in the 11- to 12-h interval it was distinctly lower than in the preceding time intervals. These conclusions are borne out in the examination of total proteins accumulating in infected cells. Thus, we noted a reduction in the accumulation of ICP8 and U_L38 protein (Fig. 3B).

Pattern of accumulation of ICP4 in the cytoplasm of cells infected with wild-type, ΔU_L41, ΔgE, or ΔgI virus. Replicate cultures of HEp-2 cells grown in four-well slides were exposed to 10 PFU of the indicated virus per cell. The cells were fixed at 2, 4, 6, 8, or 10 h after infection and stained with the ICP4 mouse monoclonal antibody, as detailed in Materials and Methods. The results from representative images shown in Fig. 4 and 5 were as follows. ICP4 was restricted to the nucleus in cells fixed at 2 and 4 h after infection. At later time intervals, the percentage of cells containing ICP4 in both the nucleus and the cytoplasm steadily increased. For example, in the ΔgE mutant virus-infected cells, the percentage of cells exhibiting ICP4 in both the nucleus and the cytoplasm increased from 58.7% to over 95% between 6 and 10 h after infection. In ΔU_L41 mutant virus-infected cells, the percentage of cells exhibiting both nuclear and cytoplasmic accumulation of ICP4 increased from 60.5% to approximately 90%. In most of the cells, the accumulated cytoplasmic ICP4 formed dense structures (Fig. 4). In contrast, ICP4 was detected in the form of diffuse fluorescence in approximately 1.6% of wild-type virus-infected cells and the number increased to approximately 10% by 10 h. Figure 5 (right panel) summarizes the results obtained at 9 h after infection for the two ΔgE mutants and the ΔgI mutant virus. In essence, while in a small fraction of wild-type virus ICP4 was exported and could be visualized as a diffuse cytoplasmic fluorescence, in the vast majority of cells infected with the ΔU_L41, ΔgE, or ΔgI mutant virus ICP4 was exported and accumulated in the cytoplasm in the form of dense aggregates. We conclude that retention of ICP4 in the nucleus re-

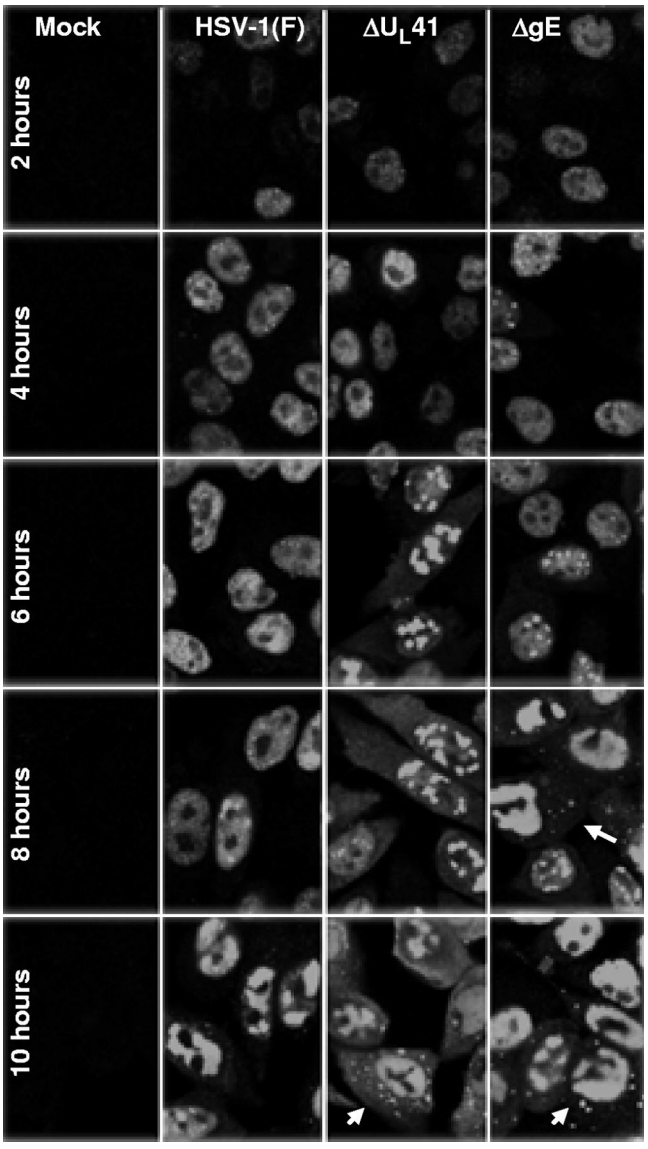

FIG. 4. Exportation of ICP4 from the nucleus and aggregation in the cytoplasm of the ΔgE and ΔU_L41 virus-infected cells. Hep-2 cells, seeded in four-well slides, were either mock infected or exposed (10 PFU/cell) to HSV-1(F), ΔgE, or ΔU_L41 mutant viruses. At 2, 4, 6, 8, or 10 h after infection, the cells were fixed in 4% paraformaldehyde and reacted with the mouse monoclonal antibody to ICP4, followed by reaction with the goat-anti mouse antibody conjugated to Alexa Fluor 488, as detailed in Materials and Methods. The images were captured with the same settings of a Zeiss confocal microscope with the aid of software provided by the manufacturer.

quires the presence in infected cells of functional gE, gI, and U_L41 protein.

Export and localization of ICP0 in the cytoplasm of infected cells. Elsewhere this laboratory reported that in cells infected with wild-type virus, ICP0 is translocated to the cytoplasm (19). The translocation is in part determined by ICP0 inasmuch as a mutant virus differing from the wild type solely in the D199A substitution in ICP0 is not translocated to the cytoplasm (52). In contrast to the diffuse appearance of ICP0 in the cytoplasm of wild-type virus-infected cells, in cells infected with a mutant lacking ICP4, ICP0 is translocated to the cytoplasm earlier and forms dense structures that include proteasomal components (28). In light of this background, it was of interest to determine the distribution of ICP0 in cells infected with the ΔU_L41, ΔgE, or ΔgI mutant virus.

In the first series of experiments, HEL cells, grown in four-well slides, were infected with wild-type or mutant viruses. The cells were fixed at 9 h after infection and reacted with anti-ICP0 antibody. The results shown in Fig. 5 (left panel) indicate that ICP0 was translocated to the cytoplasm in nearly 100% of cells infected with any one of the viruses tested. The difference between HSV-1(F) and mutant viruses centers on the appearance of ICP0. In wild-type virus-infected cells, ICP0 was diffused throughout the cytoplasm and ICP0 aggregates were found in only a very small fraction of cells. In contrast, in most cells infected with mutant viruses, ICP0 was aggregated and formed small dense structures. In cells fixed at 14 h after infection (data not shown), the aggregates were much larger, suggesting that the process continues for many hours.

The objective of the second series of experiments was based on the observation that both ICP0 and ICP4 were aggregated in the cytoplasm in mutant virus-infected cells. To test the hypothesis that the two proteins are coexported and coaggregated, HEL cells in four-well slides were infected with 10 PFU of wild-type, ΔgE, or ΔgI virus. The cells were fixed at 9 h after infection and reacted with monoclonal antibody to ICP4 and polyclonal antibody to ICP0. The results, shown in Fig. 6, were as follows. As expected, in HSV-1(F)-infected cells, ICP4 was retained in the nucleus whereas ICP0 was diffused throughout the cytoplasm (Fig. 6d to f). In both ΔgE- and ΔgI-infected cells, ICP4 was partially translocated to the cytoplasm. It appeared to be present in two forms, i.e., diffused throughout the cytoplasm and in the forms of small dense cytoplasmic structures (Fig. 6g and j). ICP0 was present in the cytoplasm, and it too appeared to be present in a diffuse form throughout the cytoplasm and in the form of small dense structures (Fig. 6h and k). In both instances, the aggregated structures of ICP0 colocalized with the structures of ICP4 (Fig. 6i and l).

We conclude that in ΔgE- or ΔgI-infected cells both ICP0 and ICP4 are translocated and colocalize, at least partly, in dense structures.

The third series of experiments centered on the nature of the small dense nuclear structure containing ICP0. To resolve this question, HEp-2 cells were harvested 18 h after infection with wild-type or ΔgE virus and processed for immunoelectron microscopy as described in Materials and Methods. The preparations were reacted with rabbit polyclonal antibody to ICP0 and anti-rabbit IgG antibody conjugated to gold. Representative images are shown in Fig. 7.

(i) In HSV-1(F)-infected cells, the predominant structures reacting with anti-ICP0 antibody were small dense structures, commonly seen in thin sections of infected cells. These structures did not appear to be enclosed in a membrane (Fig. 7A and B). In HSV-1 (F)-infected cells, these structures were detected only in nuclei.

(ii) In ΔgE mutant virus-infected cells, these structures were also present in the cytoplasm. In every respect—size, distribution, grain density, and reactivity with the ICP0 antibody—the cytoplasmic structures could not be differentiated from the nuclear structures (Fig. 7C and D).

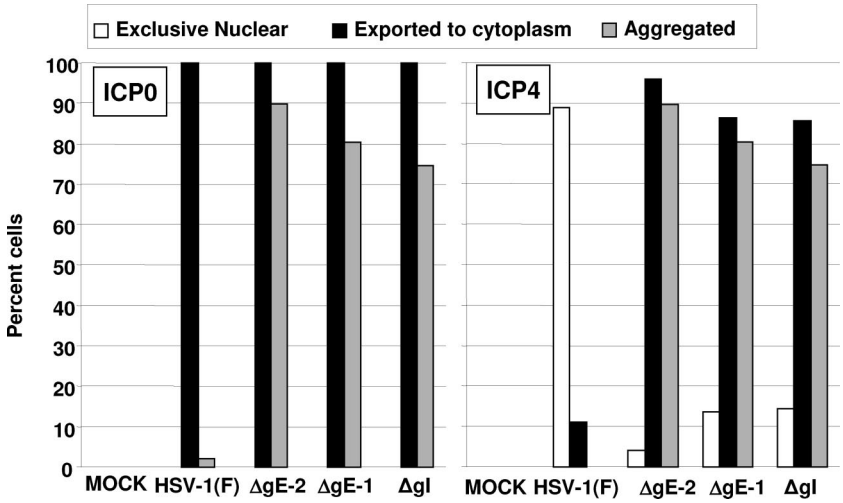

FIG. 5. Quantification of infected cells with different forms of ICP4 and ICP0. HEL cells were either mock infected or exposed (10 PFU/cell) to HSV-1(F), the ΔgE mutants (ΔgE-2 or ΔgE-1), or the ΔgI virus. The cells were fixed in 4% paraformaldehyde at 9 h after infection and doubly stained with the mouse monoclonal antibody to ICP4 and the rabbit polyclonal antibody to ICP0 exon II, followed by reactions with the goat anti-mouse Alexa Fluor 488- and the goat anti-rabbit Alexa Fluor 594-conjugated antibodies, respectively, as detailed in Materials and Methods. Approximately 200 cells from sequential fields were counted to determine the percentages of cells with exclusive nuclear ICP4 and ICP0, ICP4 and ICP0 exported to the cytoplasm, or aggregated ICP4 and ICP0. The results for each protein are presented in different plots.

(iii) ICP0 antibody also reacted, albeit less strongly, with electron opaque material at the nuclear periphery, commonly described as marginated chromatin (Fig. 7E).

(iv) Last, it has been reported that virions contain ICP0 (55). In none of the many sections examined in this study did we observe gold particles in apposition to virions either in the vicinity of the nuclear membranes or in the cytoplasmic vesicles (Fig. 7E and F). It is conceivable that the amounts of ICP0 packaged in virions are too small to be detected by this method.

Properties of the cytoplasmic structures containing ICP0 and ICP4. In wild-type virus-infected cells, ICP0 is retained in the nucleus in infected cells exposed to proteasomal inhibitors at early times (e.g., 2 h after infection). Conversely, exposure of infected cells after translocation (e.g., 9 h after infection) results in the translocation of cytoplasmic ICP0 back into the nucleus (28). Exposure of cells infected with the d120 mutant virus, lacking ICP4, at early times to proteasomal inhibitors results in nuclear retention of ICP0. Exposure to the inhibitors at late times results in aggregation of proteasomal components with ICP0 in the cytoplasm. Since in cells infected with ΔgE, ΔgI, or ΔU_L41 both ICP0 and ICP4 were translocated, the question arose as to whether the process of translocation and cytoplasmic accumulation in cells infected with these mutants is different from that taking place in cells infected with the ΔICP4 mutant virus. To resolve this question, HEL cells grown on four-well slide cultures were mock infected or exposed to 10 PFU of HSV-1(F), ΔU_L41, ΔICP4, ΔgE, or ΔgI mutant virus per cell. At 2 h after infection, a replicate set of cultures was treated with 5 μM MG132. The cells were fixed at 9 h after infection and reacted with mouse monoclonal antibody to ICP0 or rabbit polyclonal antibody to 20S proteasome core subunits. The results, shown in Fig. 8, were as follows.

As expected, in cells infected with HSV-1(F), ICP0 was translocated into the cytoplasm of untreated cells and localized in the nuclei of cells treated with the proteasome inhibitor (compare Fig. 8A, images 4 to 6, with B, images 4 to 6).

As previously reported, in cells infected with the ΔICP4 mutant virus, ICP0 was translocated to the cytoplasm and aggregated in small dense structures (28). In MG132-treated cells, ICP0 was retained in the nucleus (compare Fig. 8A, images 10 to 12, with B, images 10 to 12).

In cells infected with ΔU_L41, ΔgI, or ΔgE, as expected on the basis of data presented in this report, ICP0 was translocated to the cytoplasm and aggregated in small dense structures. In cells treated with MG132 at 2 h after infection, ICP0 was also translocated to the cytoplasm and aggregated in small dense cytoplasmic structures. In essence, in the cells infected with these mutants, MG132 failed to block the translocation of ICP0 (compare Fig. 8A, images 7 to 9, 13 to 15, and 16 to 18, with B, corresponding images).

As in the case of cells infected with the ΔU_L41, ΔgI, or ΔgE mutants and treated with proteasomal inhibitors, the antibody to the proteasomal core components reacted with the small cytoplasmic aggregates of ICP0. The antibody to the core components reacted with the surface of the aggregates and appeared to form a halo around these structures (Fig. 8). This halo effect was either too weak to be seen in or absent from untreated infected cells.

Subcellular distribution of glycoprotein E in ΔU_L41, ΔgI, and ΔgE mutant-infected cells. Published reports have shown that early after infection the gE/gI complex is sorted to the *trans*-Golgi network, whereas late in infection the complex is redistributed from the *trans*-Golgi network to other sites (4, 14, 32). During these trafficking events, the localization of other proteins may also be affected, as is the case for gE-dependent translocation of the IP3 receptor I (18). To determine whether the subcellular localization of gE is affected in ΔgI- or ΔU_L41-infected cells, HEL cells grown in four-well slides were mock infected or exposed to 10 PFU of HSV-1(F), ΔgE, ΔgI, or

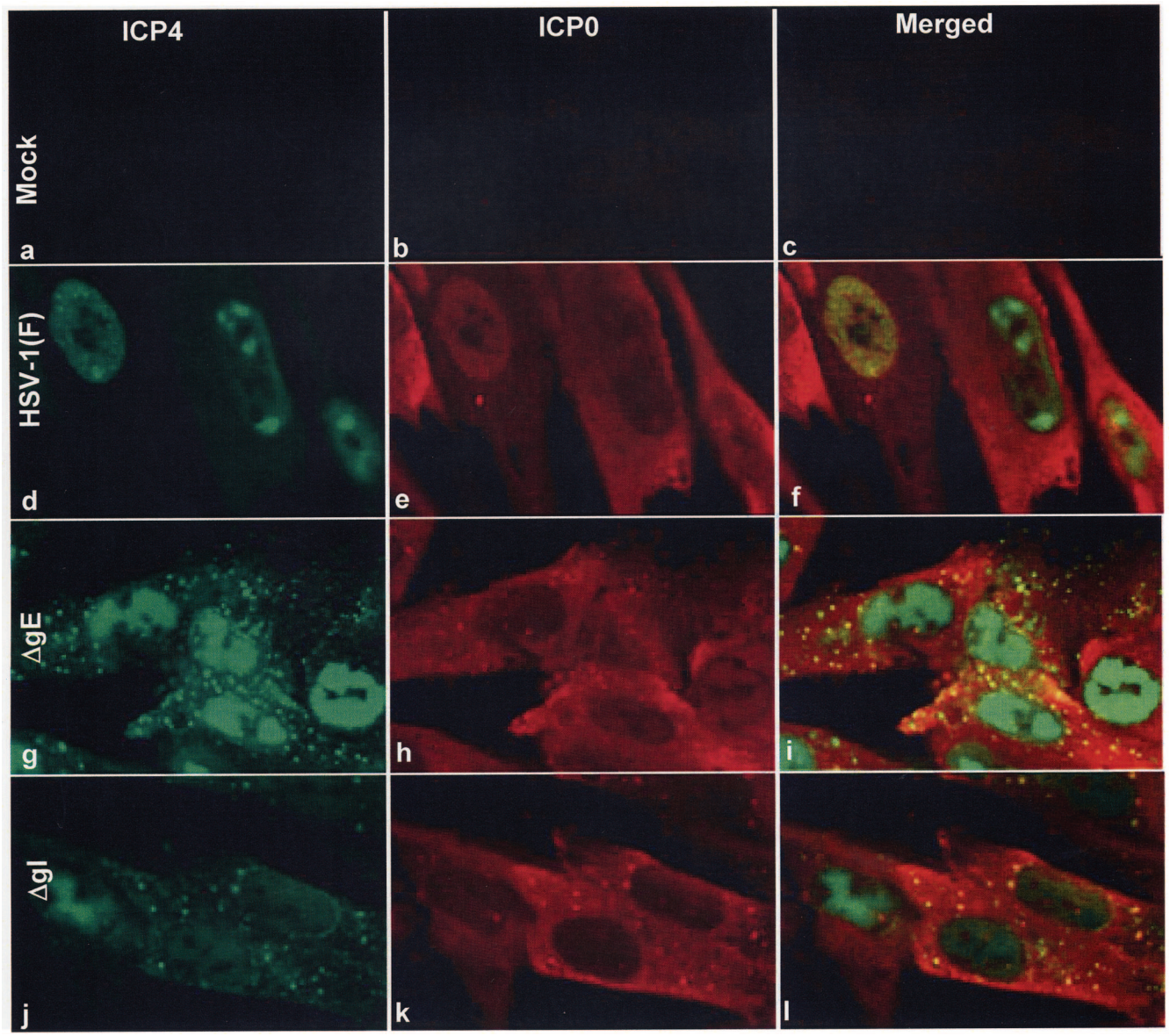

FIG. 6. Colocalization and coaggregation of ICP4 and ICP0 in the cytoplasm of ΔgE or ΔgI mutant virus-infected cells. HEL cells seeded in four-well slides were either mock infected (a, b, and c) or exposed (10 PFU/cell) to HSV-1(F) (d, e, and f), ΔgE (g, h, and i), or ΔgI (j, k, and l) mutant virus. At 9 h after infection, the cells were fixed in 4% paraformaldehyde and doubly stained with the mouse monoclonal antibody to ICP4 and the rabbit polyclonal antibody to ICP0 exon II, followed by reactions with the goat anti-mouse antibody conjugated to Alexa Fluor 488 (green fluorescence) and the goat anti-rabbit antibody conjugated to Alexa Fluor 594 (red fluorescence), respectively, as detailed in Materials and Methods. The images were captured as described in the legend to Fig. 4.

ΔU_L41 virus. The cells were fixed at 4, 8, or 12 h after infection and reacted with the anti-gE mouse monoclonal antibody and the anti-TGN46 rabbit polyclonal antibody. The results, shown in Fig. 9, were as follows. At 4 h after infection, gE was detected around the perinuclear area of all of the infected cells. The perinuclear gE protein colocalized with the *trans*-Golgi network marker TGN46. Newly synthesized protein was detected in the Golgi apparatus, on the nuclear membrane, and (diffuse) in the cytosol in all of the infected cells by 8 h after infection (data not shown). A clear difference emerged at 12 h after infection. While in most wild-type virus-infected cells gE was present in small aggregates in membranes or diffuse in the cytosol, in cells infected with either ΔgI or ΔU_L41, gE was aggregated in the *trans*-Golgi network. This network was retained in both ΔgI and ΔU_L41 mutants even late after infection. Our results indicate differences in localization of gE in cells infected with ΔgI or ΔU_L41 mutant virus and delay in the corruption of the *trans*-Golgi network compared to results for the wild-type virus-infected cells.

It should be noted that the anti-TGN46 antibody reacted with a nuclear protein at early times (4 h) after infection. This signal disappeared or was much reduced in cells reacted with the antibody at late times (12 h) after infection.

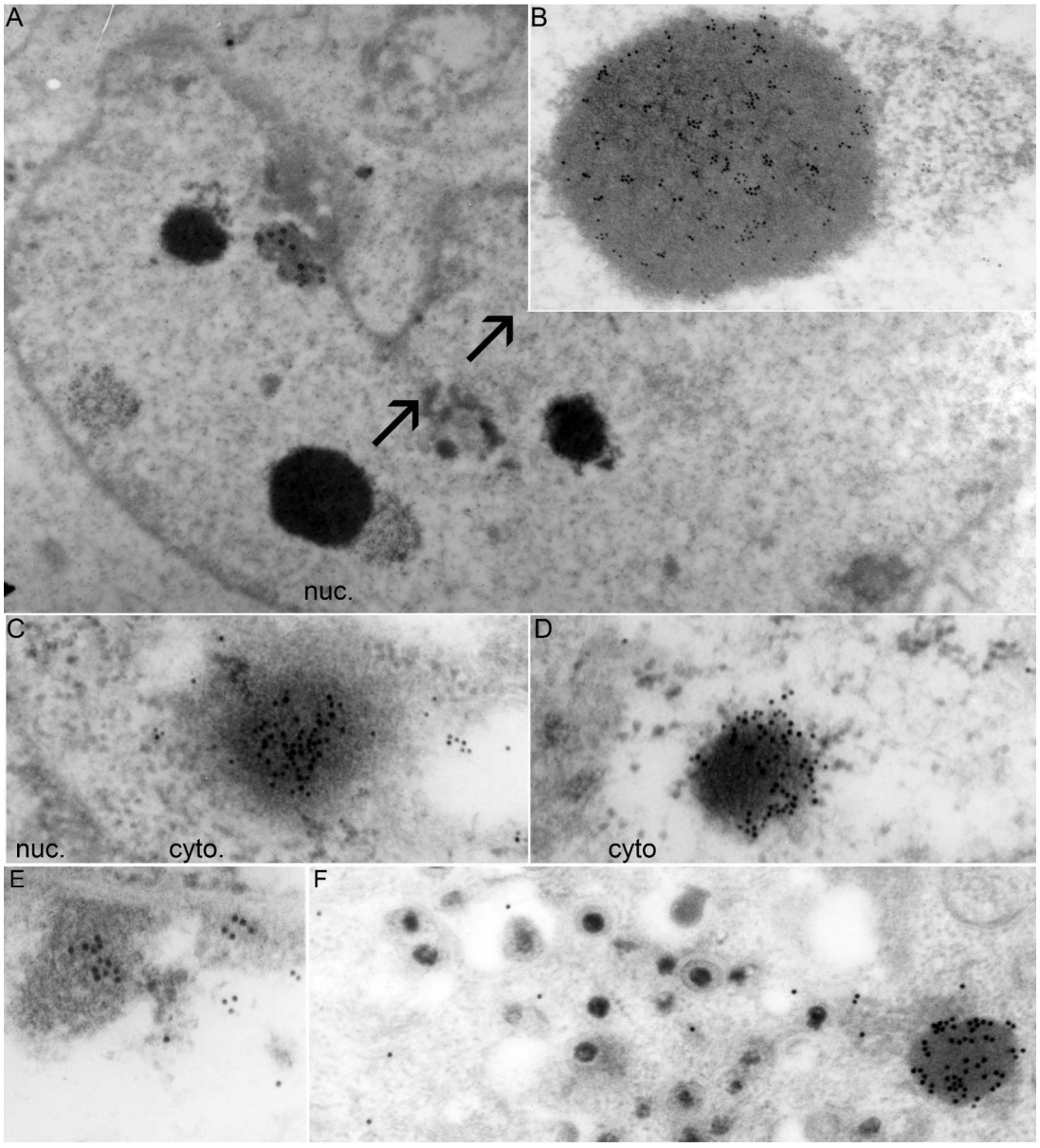

FIG. 7. Electron photomicrographs of ICP0-containing structures in HSV-1(F)- and ΔgE-infected cells. HEp-2 cells were harvested at 18 h after infection with 10 PFU/cell of HSV-1(F) or the ΔgE mutant and processed for immunoelectron microscopy, as described in Materials and Methods. Thin sections of cells were labeled with the ICP0 exon II rabbit polyclonal antibody, followed by reaction with a goat anti-rabbit IgG antibody conjugated with 10-nm colloidal gold (Ted Pella). (A) Low magnification of an HSV-1(F)-infected cell, showing a small number of electron-dense structures in the nucleus (nuc.) that contain multiple 10-nm gold particles. (B) Higher magnification of an electron-dense, gold particle-positive nuclear structure from panel A is shown with arrows. (C and D) Electron-dense structures in the cytosol of the ΔgE mutant-infected cells containing multiple 10-nm gold particles. (E) Gold particles present in association with marginated chromatin in nuclei of wild-type virus-infected cells. The density of the gold particles in the marginated chromatin was lower than that in electron-dense structures observed in the cytoplasm (cyto) of mutant virus-infected cells. (F) No gold particles were found in association with virions. In the same field, numerous gold particles were associated with electron-dense aggregates in the cytoplasm of cells infected with ΔgE virus. Control experiments involving secondary antibody conjugated to gold particles were negative (data not shown).

DISCUSSION

The salient feature of the results is that ICP4 and ICP0 are translocated to the cytoplasm and coaggregate into small dense cytoplasmic bodies in cells infected with mutant virus lacking gE, gI, or U_L41. The significance of this observation stems from several considerations. For heuristic reasons, it is convenient to summarize our knowledge of the peregrinations of ICP4 and ICP0 separately before a discussion of the present study.

(i) Foremost, ICP4 is a nuclear protein in wild-type virus-infected cells. Its function is required throughout the replicative cycle (5, 6). Translocation to the cytoplasm in the absence of gE, gI, or U_L41 protein implies that its nuclear retention is

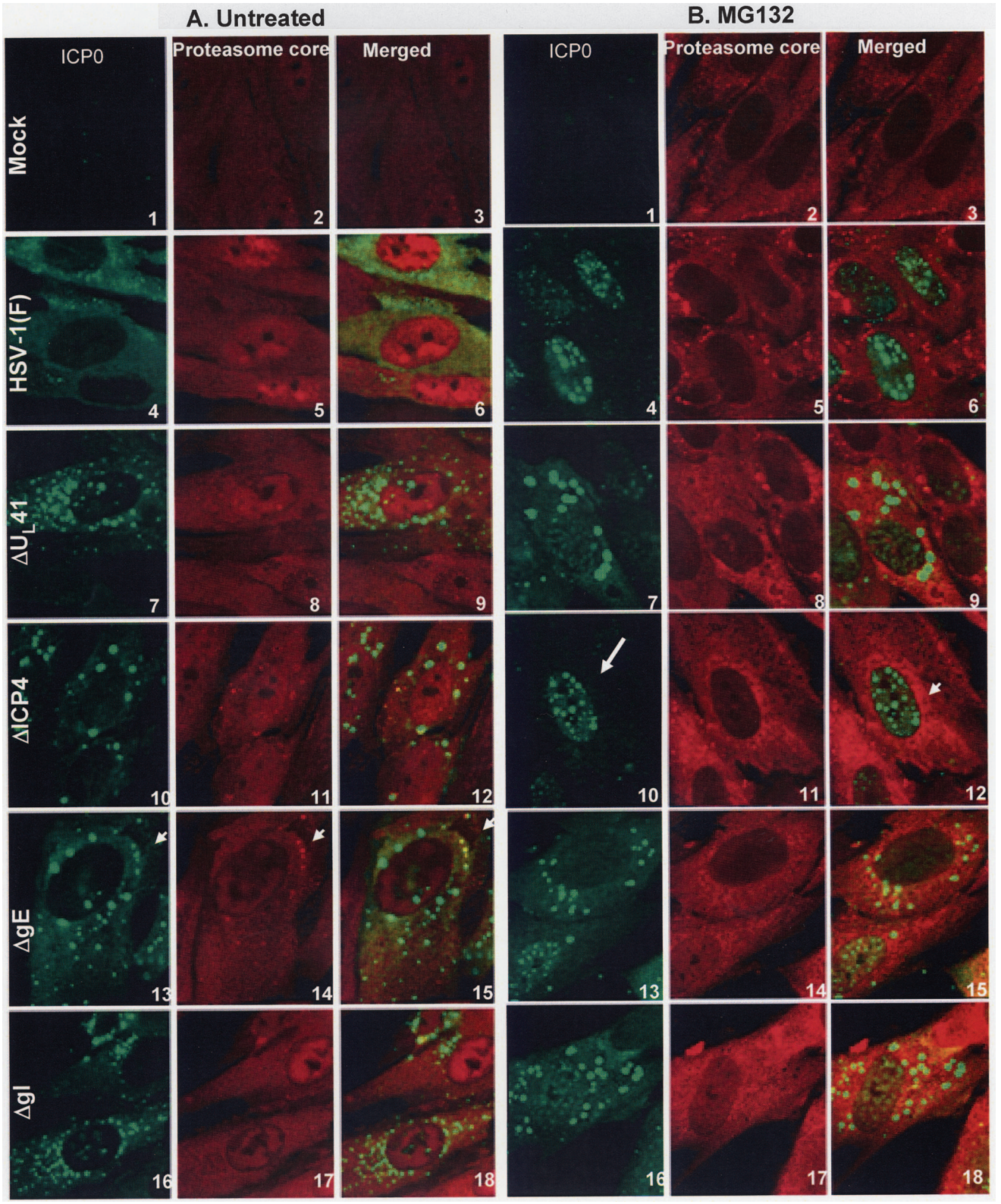

FIG. 8. Coaggregation of the ICP4/ICP0 structures with proteasomal proteins in the ΔgE, ΔgI, or ΔU_L41 mutant-infected cells. HEL cells, seeded in four-well slides, were either mock infected or exposed (10 PFU/cell) to HSV-1 (F) (A and B, images 4 to 6), ΔU_L41 (A and B, images 7 to 9), ΔICP4 (A and B, images 10 to 12), ΔgE (A and B, images 13 to 15), or ΔgI (A and B, images 16 to 18) mutant virus. At 2 h after infection, the cells were either mock treated (A, images 1 to 18) or treated with 5 μM MG132 (B, images 1 to 18). At 9 h after infection, the cells were fixed in 4% paraformaldehyde and doubly stained with the mouse monoclonal antibody to ICP0 and the rabbit polyclonal antibody to the 20S proteasome core subunits, followed by reactions with the goat anti-mouse Alexa Fluor 488- and the goat anti-rabbit Alexa Fluor 594-conjugated antibodies, as detailed in Materials and Methods. All images were captured as described in the legend to Fig. 4. Arrows (A, images 13 to 15) show the halo effect caused by reaction of the antibody to the core components with the surface of the aggregates. The arrows in panel B show the nuclear localization of ICP0 upon MG132 treatment (image 10) and aggregated proteasomal proteins (image 12).

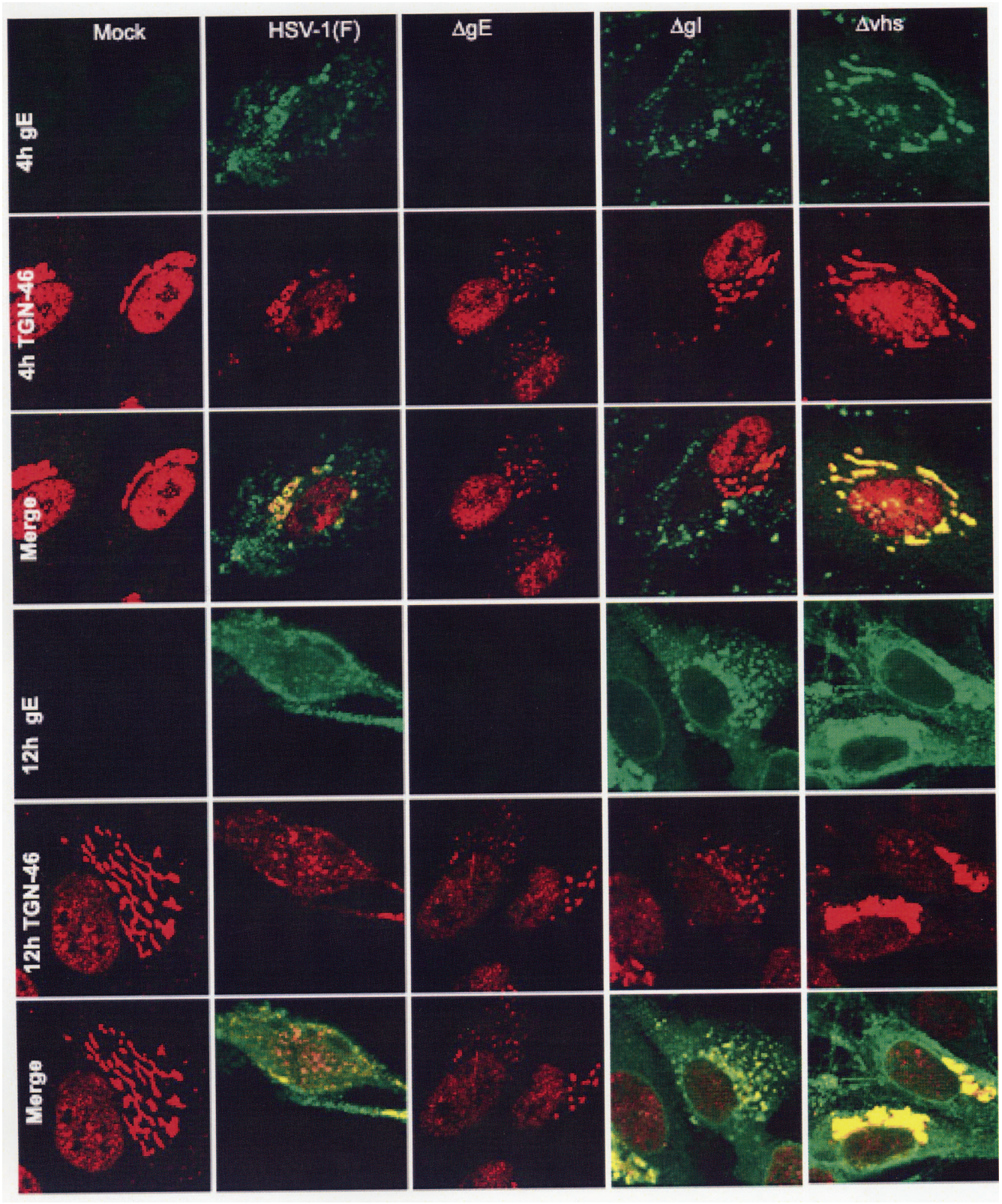

FIG. 9. Subcellular distribution of gE in the ΔU_L41 and ΔgI mutants. HEL cells, seeded in four-well slides, were exposed to 10 PFU of HSV-1(F), ΔU_L41, ΔgE, or ΔgI mutant virus per cell. At 4 or 12 h after infection, the cells were fixed in 4% paraformaldehyde and reacted with the gE mouse monoclonal antibody (clone 1108) and the TGN46 rabbit polyclonal antibody, followed by reactions with the goat anti-mouse Alexa Fluor 488 (green fluorescence)- and the goat anti-rabbit Alexa Fluor 594 (red fluorescence)-conjugated antibodies, as detailed in Materials and Methods. The images were captured as described in the legend to Fig. 4.

due to an expressed function regulated by the virus and is not due solely to the nuclear localization signal embedded in the primary structure of the protein. It is noteworthy that Zhu et al. have noted that in Vero cells both ICP0 and ICP4 encoded by the KOS strain are also detected in the cytoplasm in the form of diffuse and punctuate fluorescence (57, 58). These investigators noted that ICP4 localizes in the nucleus in the absence of ICP27 or in cells infected with certain ICP27 mutants. In contrast, coexpression of ICP27 inhibited or reduced nuclear localization of ICP4 and ICP0. The inhibitory function was mapped to the carboxyl-terminal half of ICP27 (57, 58). In more recent studies, Lengyel et al. noted that leptomycin B causes massive export of ICP4 and ICP0 from the nucleus to the cytoplasm (24). They also reported that resistance to leptomycin B maps to residues 21 to 63 in the amino-terminal domain of ICP27 (24). Interestingly, the drug has no such effect in cells infected with leptomycin B-resistant mutants. Moreover, mutants resistant to leptomycin B, including the mutants lacking residues 21 to 63 of ICP27, cannot be differentiated from wild-type viruses with respect to the ICP27 shuttling between the nucleus and cytoplasm or viral replication. The appearances of accumulated cytoplasmic ICP0 and ICP4 are different, and no suggestion of colocalization of ICP0 and ICP4 is evident from the published results. The authors suggest that the function of the amino-terminal domain of ICP27 is to export ICP0 and ICP4.

(ii) At very early stages in viral replication, ICP0 is in the nucleus, first in association with ND10 nuclear structures and later dispersed though the nucleus (12, 30, 31). ICP0 is translocated to and dispersed throughout the cytoplasm at later stages of the replicative cycle as a consequence of its dynamic association with proteasomes, inasmuch as the proteasome inhibitor MG132 blocks the translocation of ICP0 to the cytoplasm or, in cells exposed to the inhibitor later in infection, it causes the protein to be translocated back to the nucleus (16, 20). The dynamic interaction of ICP0 with proteasomal components is also apparent from the observation that in cells infected with a mutant lacking ICP4, ICP0 is translocated to the cytoplasm earlier than in cells infected with wild-type mutants (28). In contrast to ICP0 of wild-type virus-infected cells, ICP0 of mutant virus-infected cells forms dense cytoplasmic structures that, in the presence of MG132, also contain proteasomal components.

The involvement of a viral protein in the translocation process may be inferred from the observation that inhibition of DNA synthesis significantly delays but does not abolish the translocation of ICP0 (28). This observation suggests that the function is expressed by a late protein (γ_1), whose synthesis is retarded but not abolished by inhibitors of DNA synthesis. The involvement of host or viral proteins in the translocation process may also be inferred from the observation that the D199A substitution in ICP0 precludes the export of ICP0 to the cytoplasm (52, 53).

The conclusions reached by Lengyel et al. (24) and Lopez et al. (28) may in fact not be contradictory. The cotransfection studies carried out by Zhu and Schaffer suggest that ICP27 blocks the import of rather then exports ICP0 or ICP4 (58). If the studies of Lengyel et al. (24) are interpreted in the same light, it could be argued that ICP27 monitors and blocks excessive accumulation of ICP0 and ICP4 in the nucleus by sequestering the nuclear import machinery for its own use. In contrast, the translocation of ICP0 late in infection in wild-type virus-infected cells and the translocation of ICP4 and ICP0 in cells infected with the ΔgE, ΔgI, or ΔU_L41 mutant are late events and involve physical translocation of protein from the nucleus to the cytoplasm and colocalization of ICP0, ICP4, and proteasomal components. The difference between the translocation of ICP0 in wild-type virus-infected cells and that taking place in mutant virus-infected cells is that neither ICP0 nor ICP4 is reimported into the nuclei of mutant virus-infected cells following exposure to proteasomal inhibitors. The implication of this finding is that the mechanisms of translocation may be different in the two systems.

(iii) Physical interactions between ICP0 and ICP4 have been reported previously (56). This report, however, is the first report of colocalization of the proteins outside the nucleus in the context of a productive infection. It is of interest that Mullen et al. (35) reported that ICP4 and ICP0 colocalized in the cytoplasm of cells transfected with plasmids encoding wild-type ICP4 and a mutant form of ICP0 lacking residues 365 to 517 which by itself localized in the cytoplasm. The authors concluded that ICP0 dominated the interaction with ICP4 and suppressed its nuclear localization signals. Our studies involve wild-type proteins in the context of productively infected cells, with the result that the two proteins were both exported to the cytoplasm and colocalized in dense structures. Since in wild-type virus-infected cells ICP0 is translocated independently of ICP4, the question arises whether in the absence of retention signals for ICP4, ICP0 acts as a chaperone for translocation and ultimately colocalization in the dense cytoplasmic bodies.

(iv) Examination of mutant and wild-type virus-infected cells by electron microscopy with gold particle-conjugated antibody revealed that the structures containing ICP0 and by extension ICP4 were dense, amorphous protein aggregates that were not enclosed by a membrane. Of particular interest was the observation that structures virtually identical in appearance were present in the nuclei but not in the cytoplasm of wild-type virus-infected cells. Although ICP0 is largely exported from nuclei late in infection, residual small granular structures reacting with anti-ICP0 antibody continue to dot the nuclear landscape. These structures are commonly seen in thin sections of infected cell nuclei, but this is the first indication that they contain ICP0. In an earlier study (28), the question was raised whether the export of ICP0 to the cytoplasm reflects the need to sequester viral proteins that have outlived their usefulness. While the small amount of ICP0 associated with marginated chromatin may express functions needed by the virus, the function of ICP0 within the dense aggregates is less clear.

(v) Last, the question arises as to how such functionally disparate proteins, such as gE and gI, which form the Fc heterodimer and the U_L41 endoribonuclease, each independently effect the retention of ICP4 in the nucleus. We have no definitive data that bear on this question, but some aspects of the fundamental strategy of HSV-1 are relevant. Foremost, viral proteins perform several functions. Although the gE/gI complex and the U_L41 protein have been linked to shuttling between the *trans*-Golgi network and the plasma membrane and to endoribonuclease activity, respectively, it is conceivable that they perform additional functions that at this time are less well defined. The second aspect of viral strategy is to sequester

and redirect host proteins to perform novel functions. The gE/gI complex may, in the course of its shuttling activity, sequester the host protein that would be responsible for translocation of ICP4 to the cytoplasm.

Also, as noted in the introduction, there appears to be a connection between the U_L41 protein and gE. Late in the course of the replicative cycle, the U_L41 protein is neutralized by VP16 and VP22 (21, 23, 45, 49). There is ample evidence that VP22 forms complexes with a number of proteins that are ultimately packaged in virions. The assumption that this interaction occurs solely for the purpose of packaging and is not utilized by the virus for other objectives is probably incorrect. The more direct evidence of interaction may be deduced from the observation that in ΔU_L41-infected cells the accumulation of viral gene products occurs at a slower pace and in particular that the distribution of gE in ΔU_L41-infected cells lags behind that of wild-type virus-infected cells.

The notion that viral proteins are not merely directed by built-in signals or chaperoned to the nucleus but also specifically retained in the nucleus is intriguing. It overlays a novel level of regulation of viral gene functions.

ACKNOWLEDGMENTS

These studies were aided by National Cancer Institute grants CA115662, CA83939, CA71933, and CA78766.

We thank David C. Johnson of the Oregon Health Sciences University, Portland, OR, for the antibody to gE and Brunella Taddeo for helpful discussions.

REFERENCES

1. **Alconada, A., U. Bauer, and B. Hoflack.** 1996. A tyrosine-based motif and a casein kinase II phosphorylation site regulate the intracellular trafficking of the varicella-zoster virus glycoprotein I, a protein localized in the trans-Golgi network. EMBO J. **15:**6096–6110.
2. **Basu, S., G. Dubin, M. Basu, V. Nguyen, and H. M. Friedman.** 1995. Characterization of regions of herpes simplex virus type 1 glycoprotein E involved in binding the Fc domain of monomeric IgG and in forming a complex with glycoprotein I. J. Immunol. **154:**260–267.
3. **Basu, S., G. Dubin, T. Nagashunmugam, M. Basu, L. T. Goldstein, L. Wang, B. Weeks, and H. M. Friedman.** 1997. Mapping regions of herpes simplex virus type 1 glycoprotein I required for formation of the viral Fc receptor for monomeric IgG. J. Immunol. **158:**209–215.
4. **Brideau, A. D., L. W. Enquist, and R. S. Tirabassi.** 2000. The role of virion membrane protein endocytosis in the herpesvirus life cycle. J. Clin. Virol. **17:**69–82.
5. **DeLuca, N. A., M. A. Courtney, and P. A. Schaffer.** 1984. Temperature-sensitive mutants in herpes simplex virus type 1 ICP4 permissive for early gene expression. J. Virol. **52:**767–776.
6. **DeLuca, N. A., and P. A. Schaffer.** 1985. Activation of immediate-early, early, and late promoters by temperature-sensitive and wild-type forms of herpes simplex virus type 1 protein ICP4. Mol. Cell. Biol. **5:**1997–2008.
7. **Dingwell, K. S., L. C. Doering, and D. C. Johnson.** 1995. Glycoproteins E and I facilitate neuron-to-neuron spread of herpes simplex virus. J. Virol. **69:** 7087–7098.
8. **Dingwell, K. S., and D. C. Johnson.** 1998. The herpes simplex virus gE-gI complex facilitates cell-to-cell spread and binds to components of cell junctions. J. Virol. **72:**8933–8942.
9. **Duffy, C., J. H. Lavail, A. N. Tauscher, E. G. Wills, J. A. Blaho, and J. D. Baines.** 2006. Characterization of a UL49-null mutant: VP22 of herpes simplex virus type 1 facilitates viral spread in cultured cells and the mouse cornea. J. Virol. **80:**8664–8675.
10. **Ejercito, P. M., E. D. Kieff, and B. Roizman.** 1968. Characterization of herpes simplex virus strains differing in their effects on social behaviour of infected cells. J. Gen. Virol. **2:**357–364.
11. **Elliott, G., W. Hafezi, A. Whiteley, and E. Bernard.** 2005. Deletion of the herpes simplex virus VP22-encoding gene (UL49) alters the expression, localization, and virion incorporation of ICP0. J. Virol. **79:**9735–9745.
12. **Everett, R. D., and G. G. Maul.** 1994. HSV-1 IE protein Vmw110 causes redistribution of PML. EMBO J. **13:**5062–5069.
13. **Everett, R. D., A. Orr, and C. M. Preston.** 1998. A viral activator of gene expression functions via the ubiquitin-proteasome pathway. EMBO J. **17:** 7161–7169.
14. **Farnsworth, A., and D. C. Johnson.** 2006. Herpes simplex virus gE/gI must accumulate in the *trans*-Golgi network at early times and then redistribute to cell junctions to promote cell-cell spread. J. Virol. **80:**3167–3179.
15. **Farnsworth, A., T. W. Wisner, and D. C. Johnson.** 2007. Cytoplasmic residues of herpes simplex virus glycoprotein gE required for secondary envelopment and binding of tegument proteins VP22 and UL11 to gE and gD. J. Virol. **81:**319–331.
16. **Galvan, V., R. Brandimarti, J. Munger, and B. Roizman.** 2000. Bcl-2 blocks a caspase-dependent pathway of apoptosis activated by herpes simplex virus 1 infection in HEp-2 cells. J. Virol. **74:**1931–1938.
17. **Jacobs, L.** 1994. Glycoprotein E of pseudorabies virus and homologous proteins in other alphaherpesvirinae. Arch. Virol. **137:**209–228.
18. **Kalamvoki, M., and B. Roizman.** 2007. Bcl-2 blocks accretion or depletion of stored calcium but has no effect on the redistribution of IP3 receptor I mediated by glycoprotein E of herpes simplex virus 1. J. Virol. **81:**6316–6325.
19. **Kawaguchi, Y., R. Bruni, and B. Roizman.** 1997. Interaction of herpes simplex virus 1 alpha regulatory protein ICP0 with elongation factor 1delta: ICP0 affects translational machinery. J. Virol. **71:**1019–1024.
20. **Kawaguchi, Y., C. Van Sant, and B. Roizman.** 1997. Herpes simplex virus 1 alpha regulatory protein ICP0 interacts with and stabilizes the cell cycle regulator cyclin D3. J. Virol. **71:**7328–7336.
21. **Knez, J., P. T. Bilan, and J. P. Capone.** 2003. A single amino acid substitution in herpes simplex virus type 1 VP16 inhibits binding to the virion host shutoff protein and is incompatible with virus growth. J. Virol. **77:**2892–2902.
22. **Kwong, A. D., and N. Frenkel.** 1987. Herpes simplex virus-infected cells contain a function(s) that destabilizes both host and viral mRNAs. Proc. Natl. Acad. Sci. USA **84:**1926–1930.
23. **Lam, Q., C. A. Smibert, K. E. Koop, C. Lavery, J. P. Capone, S. P. Weinheimer, and J. R. Smiley.** 1996. Herpes simplex virus VP16 rescues viral mRNA from destruction by the virion host shutoff function. EMBO J. **15:** 2575–2581.
24. **Lengyel, J., A. K. Strain, K. D. Perkins, and S. A. Rice.** 2006. ICP27-dependent resistance of herpes simplex virus type 1 to leptomycin B is associated with enhanced nuclear localization of ICP4 and ICP0. Virology **352:**368–379.
25. **Leopardi, R., and B. Roizman.** 1996. The herpes simplex virus major regulatory protein ICP4 blocks apoptosis induced by the virus or by hyperthermia. Proc. Natl. Acad. Sci. USA **93:**9583–9587.
26. **Longnecker, R., S. Chatterjee, R. J. Whitley, and B. Roizman.** 1987. Identification of a herpes simplex virus 1 glycoprotein gene within a gene cluster dispensable for growth in cell culture. Proc. Natl. Acad. Sci. USA **84:**4303–4307.
27. **Longnecker, R., and B. Roizman.** 1987. Clustering of genes dispensable for growth in culture in the S component of the HSV-1 genome. Science **236:** 573–576.
28. **Lopez, P., C. Van Sant, and B. Roizman.** 2001. Requirements for the nuclear-cytoplasmic translocation of infected-cell protein 0 of herpes simplex virus 1. J. Virol. **75:**3832–3840.
29. **Lubinski, J., T. Nagashunmugam, and H. M. Friedman.** 1998. Viral interference with antibody and complement. Semin. Cell Dev. Biol. **9:**329–337.
30. **Maul, G. G., and R. D. Everett.** 1994. The nuclear location of PML, a cellular member of the C3HC4 zinc-binding domain protein family, is rearranged during herpes simplex virus infection by the C3HC4 viral protein ICP0. J. Gen. Virol. **75:**1223–1233.
31. **Maul, G. G., H. H. Guldner, and J. G. Spivack.** 1993. Modification of discrete nuclear domains induced by herpes simplex virus type 1 immediate early gene 1 product (ICP0). J. Gen. Virol. **74:**2679–2690.
32. **McMillan, T. N., and D. C. Johnson.** 2001. Cytoplasmic domain of herpes simplex virus gE causes accumulation in the *trans*-Golgi network, a site of virus envelopment and sorting of virions to cell junctions. J. Virol. **75:**1928–1940.
33. **Meignier, B., R. Longnecker, P. Mavromara-Nazos, A. E. Sears, and B. Roizman.** 1988. Virulence of and establishment of latency by genetically engineered deletion mutants of herpes simplex virus 1. Virology **162:**251–254.
34. **Miriagou, V., L. Stevanato, R. Manservigi, and P. Mavromara.** 2000. The C-terminal cytoplasmic tail of herpes simplex virus type 1 gE protein is phosphorylated in vivo and in vitro by cellular enzymes in the absence of other viral proteins. J. Gen. Virol. **81:**1027–1031.
35. **Mullen, M. A., S. Gerstberger, D. M. Ciufo, J. D. Mosca, and G. S. Hayward.** 1995. Evaluation of colocalization interactions between the IE110, IE175, and IE63 transactivator proteins of herpes simplex virus within subcellular punctate structures. J. Virol. **69:**476–491.
36. **Nagashunmugam, T., J. Lubinski, L. Wang, L. T. Goldstein, B. S. Weeks, P. Sundaresan, E. H. Kang, G. Dubin, and H. M. Friedman.** 1998. In vivo immune evasion mediated by the herpes simplex virus type 1 immunoglobulin G Fc receptor. J. Virol. **72:**5351–5359.
37. **Ng, T. I., W. O. Ogle, and B. Roizman.** 1998. UL13 protein kinase of herpes simplex virus 1 complexes with glycoprotein E and mediates the phosphorylation of the viral Fc receptor: glycoproteins E and I. Virology **241:**37–48.
38. **O'Regan, K. J., M. A. Bucks, M. A. Murphy, J. W. Wills, and R. J. Courtney.** 2007. A conserved region of the herpes simplex virus type 1 tegument protein

VP22 facilitates interaction with the cytoplasmic tail of glycoprotein E (gE). Virology **358:**192–200.

39. **Penfold, M. E., P. Armati, and A. L. Cunningham.** 1994. Axonal transport of herpes simplex virions to epidermal cells: evidence for a specialized mode of virus transport and assembly. Proc. Natl. Acad. Sci. USA **91:**6529–6533.
40. **Polcicova, K., K. Goldsmith, B. L. Rainish, T. W. Wisner, and D. C. Johnson.** 2005. The extracellular domain of herpes simplex virus gE is indispensable for efficient cell-to-cell spread: evidence for gE/gI receptors. J. Virol. **79:** 11990–12001.
41. **Poon, A. P., and B. Roizman.** 1997. Differentiation of the shutoff of protein synthesis by virion host shutoff and mutant gamma (1)34.5 genes of herpes simplex virus 1. Virology **229:**98–105.
42. **Post, L. E., A. J. Conley, E. S. Mocarski, and B. Roizman.** 1980. Cloning of reiterated and nonreiterated herpes simplex virus 1 sequences as BamHI fragments. Proc. Natl. Acad. Sci. USA **77:**4201–4205.
43. **Post, L. E., and B. Roizman.** 1981. A generalized technique for deletion of specific genes in large genomes: alpha gene 22 of herpes simplex virus 1 is not essential for growth. Cell **25:**227–232.
44. **Sciortino, M. T., B. Taddeo, M. Giuffre-Cuculletto, M. A. Medici, A. Mastino, and B. Roizman.** 2007. Replication-competent herpes simplex virus 1 isolates selected from cells transfected with a bacterial artificial chromosome DNA lacking only the UL49 gene vary with respect to the defect in the UL41 gene encoding host shutoff RNase. J. Virol. **81:**10924–10932.
45. **Smibert, C. A., B. Popova, P. Xiao, J. P. Capone, and J. R. Smiley.** 1994. Herpes simplex virus VP16 forms a complex with the virion host shutoff protein vhs. J. Virol. **68:**2339–2346.
46. **Smiley, J. R.** 2004. Herpes simplex virus virion host shutoff protein: immune evasion mediated by a viral RNase? J. Virol. **78:**1063–1068.
47. **Sprague, E. R., C. Wang, D. Baker, and P. J. Bjorkman.** 2006. Crystal structure of the HSV-1 Fc receptor bound to Fc reveals a mechanism for antibody bipolar bridging. PLoS Biol. **4:**e148.
48. **Strom, T., and N. Frenkel.** 1987. Effects of herpes simplex virus on mRNA stability. J. Virol. **61:**2198–2207.
49. **Taddeo, B., M. T. Sciortino, W. Zhang, and B. Roizman.** 2007. Interaction of herpes simplex virus RNase with VP16 and VP22 is required for the accumulation of the protein but not for accumulation of mRNA. Proc. Natl. Acad. Sci. USA **104:**12163–12168.
50. **Taddeo, B., W. Zhang, and B. Roizman.** 2006. The U(L)41 protein of herpes simplex virus 1 degrades RNA by endonucleolytic cleavage in absence of other cellular or viral proteins. Proc. Natl. Acad. Sci. USA **103:**2827–2832.
51. **Tirabassi, R. S., R. A. Townley, M. G. Eldridge, and L. W. Enquist.** 1998. Molecular mechanisms of neurotropic herpesvirus invasion and spread in the CNS. Neurosci. Biobehav. Rev. **22:**709–720.
52. **Van Sant, C., Y. Kawaguchi, and B. Roizman.** 1999. A single amino acid substitution in the cyclin D binding domain of the infected cell protein no. 0 abrogates the neuroinvasiveness of herpes simplex virus without affecting its ability to replicate. Proc. Natl. Acad. Sci. USA **96:**8184–8189.
53. **Van Sant, C., P. Lopez, S. J. Advani, and B. Roizman.** 2001. Role of cyclin D3 in the biology of herpes simplex virus 1 ICP0. J. Virol. **75:**1888–1898.
54. **Wisner, T., C. Brunetti, K. Dingwell, and D. C. Johnson.** 2000. The extracellular domain of herpes simplex virus gE is sufficient for accumulation at cell junctions but not for cell-to-cell spread. J. Virol. **74:**2278–2287.
55. **Yao, F., and R. J. Courtney.** 1992. Association of ICP0 but not ICP27 with purified virions of herpes simplex virus type 1. J. Virol. **66:**2709–2716.
56. **Yao, F., and P. A. Schaffer.** 1994. Physical interaction between the herpes simplex virus type 1 immediate-early regulatory proteins ICP0 and ICP4. J. Virol. **68:**8158–8168.
57. **Zhu, Z., W. Cai, and P. A. Schaffer.** 1994. Cooperativity among herpes simplex virus type 1 immediate-early regulatory proteins: ICP4 and ICP27 affect the intracellular localization of ICP0. J. Virol. **68:**3027–3040.
58. **Zhu, Z., and P. A. Schaffer.** 1995. Intracellular localization of the herpes simplex virus type 1 major transcriptional regulatory protein, ICP4, is affected by ICP27. J. Virol. **69:**49–59.